



Why state-of-the-art analytical models for eddy current losses in PM of PMSM are insufficient for variable speed motors

Mike Königs · Bernd Löhlein

Received: 26 September 2023 / Accepted: 8 February 2024 / Published online: 12 March 2024
 © The Author(s) 2024

Abstract This is the third paper in a series on novel methods for calculating eddy current losses in permanent magnets (PM) and the shortcomings of previously conducted analyses. In the first paper, Ruoho's work on homogeneous materials was discussed. The distribution of fields has been expanded to include the reaction field of the eddy currents within the permanent magnets. This approach was based on the methods of the harmonic complex AC calculation. In the second paper, the models were expanded to enable a harmonic calculation of eddy current losses in permanent magnets for homogeneous fields including the effects of eddy current losses in an adjacent ferromagnetic material, leakage flux factors, and source behavior. In this third and final publication, a look at state-of-the-art analytical models will be taken. With regard to the results of the second publication of this series, it can be shown that established analytical models are insufficient when calculating inverter-related eddy current losses in permanent magnets of permanent magnet synchronous machines (PMSM). Furthermore, a short introduction to eddy current loss mechanics in permanent magnets of PMSM will be given.

Keywords Permanent magnet · Eddy current · Eddy current losses · Segmentation · High-speed motor · Inverter-related losses

Warum aktuelle analytische Berechnungsmodelle für die Berechnung von Wirbelstromverlusten in PM von PMSM bei Umrichterbetrieb unzureichend sind

Zusammenfassung Dies ist die dritte und letzte Veröffentlichung in einer Reihe über eine neuartige Methode für die Berechnung von Wirbelstromverlusten in Permanentmagneten (PM) und die Limitierungen bisheriger Berechnungsverfahren. In der ersten Veröffentlichung wurde die Arbeit von Ruoho für homogene Feldverteilungen erweitert, um die Feldrückwirkung des Wirbelstromes im Permanentmagneten zu berücksichtigen. Dieser Ansatz basierte auf den Methoden der komplexen Wechselstromrechnung. In der zweiten Veröffentlichung wurde das Modell erweitert, um die Einflüsse der Blechpakete, Streuflüsse und des Quellenverhaltens zu berücksichtigen und zu quantifizieren. In dieser dritten und letzten Veröffentlichung wird gezeigt, dass etablierte analytische Modelle Annahmen treffen, die in Retroperspektive nicht zulässig sind. Die Modelle sind damit nicht hinreichend für die Berechnung von Wirbelstromverlusten in PM bei Umrichterbetrieb. Weiters wird ein kurzer Einblick in die Verlustmechaniken in Permanentmagneten in PMSM gegeben.

Schlüsselwörter Permanentmagnet · Wirbelstrom · Wirbelstromverluste · Segmentierung · Schnelldrehende Antriebe · Umrichterbedingte Verluste

1 Introduction

Eddy current loss and its mitigation are major considerations in the design of high-speed motors in the automotive sector. In electric car drive trains, choke inductances are rarely used to reduce the number of

M. Königs · B. Löhlein (✉)
 Institut für Innovative Antriebstechnik, University of Applied
 Sciences Flensburg, Kanzleistraße 91-93, 24943 Flensburg,
 Germany
 bernd.loehlein@hs-flensburg.de

components. However, this increases the inverter-related current ripple and, therefore, the eddy current loss in the rotor of electric machines. The additional energy input increases the thermal load on the magnets, which can deteriorate their magnetic properties and cause permanent demagnetization of the permanent magnets in a permanent magnet synchronous machine (PMSM). Several analytical models have been developed in recent years as an alternative to time-consuming 3-D FEM co-simulations. This publication discusses the hypothesis that the analytical models known to the authors are insufficient for calculating inverter-related losses. The foundation for this discussion was established in previous publications in this series. The first publication [5] introduces the model used for the analysis, while the second publication [6] investigates the influence factors on segmentation effectiveness for harmonic homogeneous flux distributions. It is shown that the characteristics of the source are a major factor in the behavior of the segmentation effectiveness. In state-of-the-art analytical models, there is no option for the characterization of the source of magnetic flux. This publication investigates whether this oversight is a valid simplification in electrical machines. Firstly, the reasons for eddy current loss in PM of PMSM are introduced.

2 Eddy current losses in PM of PMSM

First of all, the three main source mechanisms of eddy current losses in the PM of PMSM are discussed. An ideal synchronous machine should only have a flux component that rotates synchronously with the rotor, creating no change in flux distribution in the rotor coordinate system over time. However, the discrete localization of windings and teeth generates harmonics that are observable in the rotor system.

2.1 Slot harmonics

Even without any current in the winding, the magnetic reluctance changes under the teeth and slots of the stator, which alters the working point of the permanent magnet. This change in working point results in a change in flux density, inducing a voltage that creates eddy currents in the permanent magnet and surrounding electrically conductive materials. The effect of the permanent magnet's proximity to the slots is more pronounced in SPM due to the generation of a large local flux deviation. However, this effect is not significant with IPM. The fundamental frequency of the slot harmonics is calculated based on the rotational speed n and the number of slots N_1 , with higher harmonics being prevalent. The slot harmonic frequencies follow Eq. (1) with k being an integer num-

ber. In case of symmetry (no unsymmetric saturation effects under load), k is limited to odd integers.

$$f_{\text{slot}} = n \cdot N_1 \cdot k \quad (1)$$

It is important to note that the flux deviation is not uniformly distributed over the magnet.

2.2 Winding harmonics

With sinusoidal currents, the discrete nature of the slots causes winding harmonics. The simplified rectangular representation of the field excitation curve shows that harmonics are present in the field generated by the stator winding. The resulting flux distributions are related to the number of stator slots N_1 . In case of the winding harmonics sub harmonics can exist. An exemplary derivation is given in Appendix 1.

$$f_{\text{winding}} = n \cdot N_1 \cdot k \quad (2)$$

2.3 Inverter-related losses

Synchronous machines are commonly used as variable-speed motors. This is achieved by utilizing voltage source inverters and modulating a DC link voltage using pulse width modulation (PWM). The fundamental harmonic of the modulated voltage is then used as the fundamental frequency of the motor. However, the higher harmonics in the signal, particularly the pulse frequency of the inverter, generate additional current ripple to the sinusoidal base current. The current ripple causes a change in flux density in the rotor, resulting in significant eddy current losses. The main frequencies of inverter-related losses are the pulse frequency of the inverter, its sidebands based on the fundamental frequency, and its higher order harmonics in the stator reference frame [12, 13]. Under the assumption that the inverter switching frequency is much higher than the fundamental frequency of the drive, the rotation can be neglected and the frequencies of the magnetic flux can be estimated by using Eq. (3). A general description of inverter-related harmonics can be found in [12].

$$f_{\text{inv}} = k_p \cdot f_{\text{pulse}} \pm m \cdot n \cdot p \quad (3)$$

where $k_p \in \mathbb{N}$ and $m \in \mathbb{N}$.

2.4 Loss distribution in electrical motors

To quantify the impacts of the three major loss distributions, 2-D FEM simulations were conducted. The hypothesis was that inverter-related losses constitute a significant portion of eddy current losses in the permanent magnet of the PMSM. Therefore, a SPM motor-topology with a large number of winding harmonics was chosen. Servomotors with

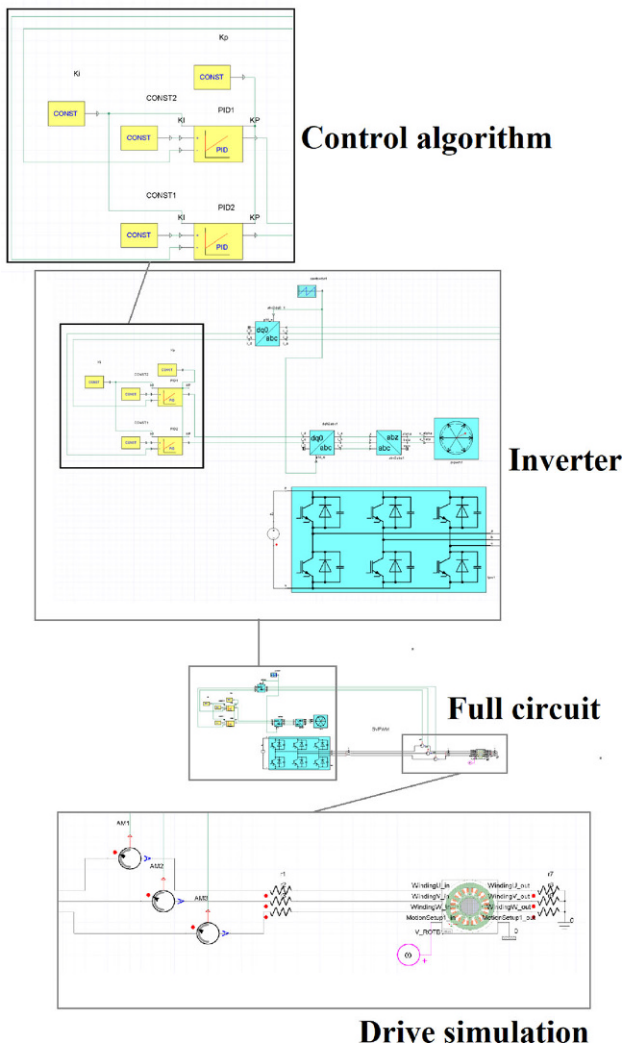


Fig. 1 Simulation circuit for FEM cosimulation

concentrated windings, or tooth coil windings, produce an extensive amount of winding harmonics. The simulation was conducted using Ansys Electronic Desktop 2022R2. It includes a 2D model of the electric motor and a circuit that models the voltage source inverter. The inverter voltage signal is directly fed into the machine model, creating a co-simulation. To implement a field-oriented control, the inverter uses space vector modulation and a PI controller. Fig. 1 shows the circuit.

A cross section of the selected motor design is shown in Fig. 2. The corresponding machine parameters are listed in Table 1.

A high inverter switching frequency, such as 64 kHz used in inverters with the new wide bandgap semiconductor technology, should theoretically reduce the inverter-related losses in the PMSM. Therefore, the the combination of a motor design with concentrated windings and a high inverter switching frequency should be one of the cases where the proportion of inverter-related losses in the permanent magnet

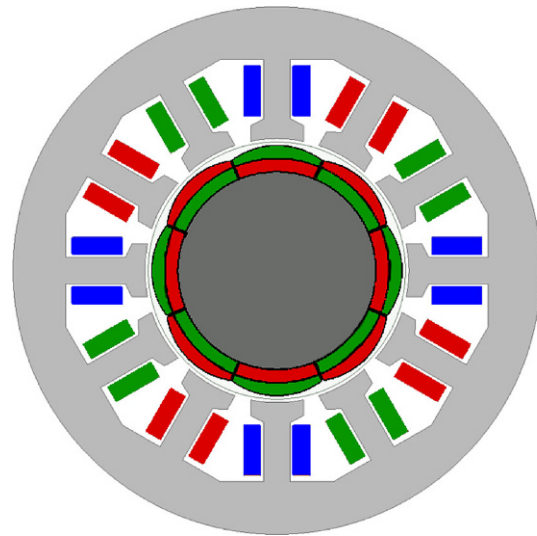


Fig. 2 Cross section of the considered servomotor with concentrated winding

should be the lowest. To estimate the proportions of losses due to slot harmonics, winding harmonics, and inverter-related losses, the machine is first simulated in no-load operation. This results in the computation of the eddy current losses in the PM due to slot harmonics. The ideal sinusoidal load case results in eddy current losses in the PM due to slot and winding harmonics. Although the superposition of powers is not valid, the losses associated with winding harmonics can be approximated by subtracting the slot harmonics from the no-load simulation from the ideal load results. This is done to offer an approximate insight into the magnitude at which winding design can reduce eddy current loss in PM of PMSM. The same is done for inverter related losses. The simulation is performed with a co-simulation of the inverter and the machine. The total eddy current losses consist of losses due to slot harmonics, winding harmonics and inverter related losses. The separate losses for the machine at a switching frequency of 64 kHz and 16 kHz at 3000 min^{-1} and 6000 min^{-1} under a load of 3.9 Nm are shown in Fig. 3. At 16 kHz the inverter-related losses are significantly higher. Due to the higher induced voltage at higher rotational speeds, the inverter-related losses are decreased at higher speeds.

Table 1 Machine Parameters PMSM

Number of polepairs	p	4
Number of stator slots	N_1	12
Outer machine diameter	d_m	80 mm
Axial length	l_m	60 mm
Rated torque	M	3.9 Nm
Magnetomotive force per tooth	Θ	360 A
DC-link voltage	U_{DC}	565 V
Inverter switching frequency	f_{pulse}	64 kHz

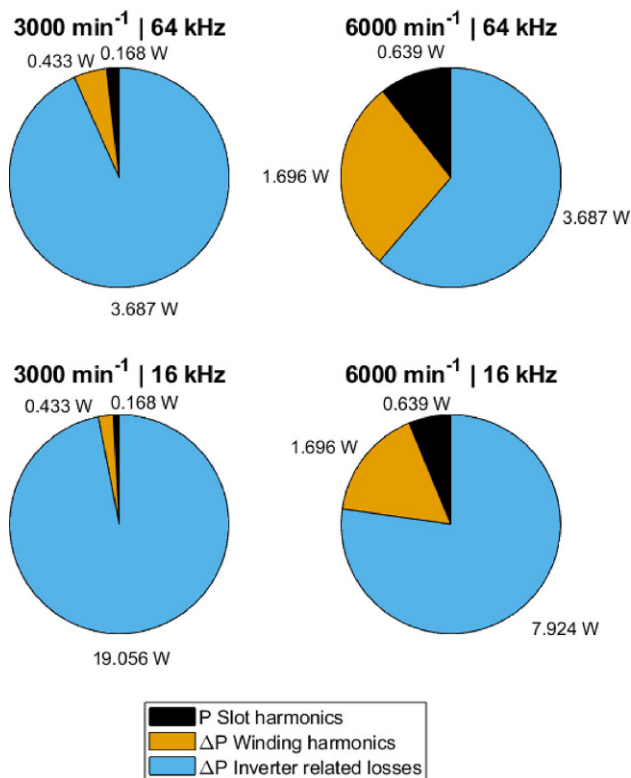


Fig. 3 Separation of eddy current loss changes in the PMs based on their cause at two different speeds and pulse frequencies

It can be deduced that, even in one of the cases where the inverter-related losses should contribute to lowest portion of losses, the inverter-related losses contribute the major part of the eddy current losses in the permanent magnets of the PMSM.

3 Source characteristics and analytic models

3.1 Source characteristics for eddy current loss calculations

In the previous publication [6] it was shown that modeling the source can significantly change the segmentation behavior and the calculated eddy current losses in permanent magnets of PMSM. In the following paragraph, the reasons for eddy current losses in PM of PMSM discussed in Sect. 2 will be examined with a focus on the necessary modeling assumptions. The starting point will be magnetic flux. Most analytical approaches to the calculation of eddy current losses start with the magnetic flux density distribution in the exposed material. In the simplest case, the calculation is based only on Faraday's law of induction and ohmic resistance, neglecting any flux generated by the eddy currents themselves. For high material resistivity and low frequencies, this approach is approximately correct. As the material becomes more conductive and frequencies increase, most analytical models superimpose a flux opposite to the excitation flux that dis-

places some of the eddy currents. As a result, the total flux decreases. This is equivalent to an excitation coil carrying a constant current.

3.1.1 Slot harmonics

Permanent magnets can be modelled using an Amperian equivalent circuit, where they carry a constant current dependent on their coercivity. The flux changes locally due to the change in reluctance caused by rotation. The excitation current linkage remains constant, but the total flux is subject to change. Therefore, it is valid to model the excitation flux density and use the superposition principle to account for the eddy current reaction flux. The model must consider the different factors that affect the formation of reaction flux. The flux linkage remains constant while the total magnetic flux changes.

3.1.2 Winding harmonics

The control of winding harmonics in variable-speed motors is also important. It is necessary to control the current in the winding using the voltage source inverter to ensure that the fundamental frequency component remains constant during constant operation. It is important to note that the excitation flux linkage in the rotating DQ-reference frame remains constant with sinusoidal currents. A model that accounts for winding harmonics can use the flux density distribution in the permanent magnet and should use parameters to calculate the eddy current reaction flux. The excitation current linkage remains constant while the total magnetic flux changes. However, in line-operated motors, this assumption no longer holds.

3.1.3 Inverter-related losses

Regarding inverter-related losses, the model needs to provide additional information about the source. Inverter-related losses occur due to an impressed voltage, not an impressed current. Assuming the coil's resistance is negligible, the total flux linkage's derivation over time is equal to the voltage on the coil terminals. Despite inverter-related losses, the total flux remains constant, while the current linkage changes due to reaction flux. Therefore, it is not allowed to use the flux distribution of the no eddy current load and superimpose the reaction flux. Furthermore, the characteristics of eddy current losses are significantly affected by coil leakage flux or choke inductances, which must be taken into account in the model.

3.2 Yamazaki et al. [1, 2]

Yamazaki et al. use a formula to calculate eddy current losses in a conductor in a uniform magnetic field given in a Japanese book[3]. The formula uses the skin depth in a homogeneous environment, which cannot account for the function of reluctance in the 3D space of a real machine. The equation is based on the external magnetic field strength. The results in Yamazaki's

Fig. 12 [1] agree with the flux impressed analysis models given in [5]. As mentioned in previous sections, the approach of an external field with the superposition of the eddy current reaction flux is valid for current-based sources such as slot and winding harmonics, but is not sufficient for inverter-related losses because the external field changes based on the reaction flux.

3.3 Sahu et al. [4]

Sahu et al. used the method of images to solve the diffusion equation. This is based on the assumption that a known external field strength H is added. The total field strength is then calculated:

$$H = H_{\text{ext}} + H_{\text{rea}} \quad (4)$$

Where H_{ext} is the external excitation field and H_{rea} is the magnetic field strength of the eddy current in the permanent magnet. A constant external magnetic field strength as excitation is equivalent to a current impressed source. Similar to Yamazaki's studies, this will work well for slot and winding harmonics, still neglecting the spatial distribution of the reluctance for the reaction flux, but neglecting the different source characteristics of the inverter-related losses.

3.4 Bettayeb et al. [7, 8]

Bettayeb et al. use multiple variants. They neglect reaction flux in some cases and consider formulas for wide but thin conductors in others. However, similar to Yamazaki et al. and Sahu et al., their calculations are based on the magnetic field distribution and do not consider source modeling.

3.5 Mirzaei et al. [10]

Mirzaei et al. present a model that can account for both, the inclusion and the exclusion of reaction flux. The model is based on the distribution of the field and, like the previously discussed models, is useful for defined current excitation. To accurately compute the reaction flux, the airgap is taken into consideration. The analysis of both, with and without eddy current reaction flux, provides boundaries for the actual losses while considering voltage-impressed inverter-related eddy currents. The model is limited to flux distributions in one direction, specifically radial for radial flux machines. As a result, it may not accurately represent machines with very thick surface-mounted permanent magnets, such as those with Halbach arrays.

3.6 Bode et al. [11]

Bode et al. present a quasi-3D algorithm that utilizes the magnetic vector potential to calculate losses based on the Poynting vector. The algorithm also

considers the flux distribution and superimposes the reaction flux to reduce the total flux linkage. The issue with voltage-impressed inverter-related losses with constant flux linkage prevails as in the previous presented publications.

3.7 Ede et al. [9]

Ede et al. assume resistance-limited eddy currents and do not consider any reaction flux. Therefore, the total flux linkage remains constant. Although reaction flux contributes to the eddy current displacement in permanent magnets, the results of the Ede's model may be more reliable. In conventional machines, slot and winding harmonics typically have much lower frequency components compared to inverter switching frequencies. The impact of reaction flux on lower frequencies is significantly lower, which reduces the error caused by neglecting reaction flux. Ignoring reaction flux keeps the total flux linkage constant with regard to inverter-related losses. If current displacement effects are not considered, the losses will be higher compared to the physical system. However, this approach is on the pessimistic side, which allows for a safe design. When the system is coupled with a choke inductance or has high leakage inductance, inaccuracies increase. This suggests a need for segmentation, even when it may not seem necessary.

4 FEM simulations with various source models

4.1 FEM Simulation

To provide an understanding of the effects of model building assumptions, FEM simulations were performed using various excitation strategies. Due to time constraints, the simulations were limited to 2D models. The considered machine is a high-speed PMSM with rotational speeds of up to $20\,000\text{ min}^{-1}$. Some of the machine's parameters are listed in Table 2.

The setup for the voltage source inverter used in this case is equivalent to the voltage source inverter introduced in Subsect. 2.4. However, three geometrically identical motors are simulated simultaneously with a different simulation setup. Firstly, the inverter

Table 2 Machine parameters, PMSM with concentrated winding

Number of polepairs	p	2
Number of stator slots	N_1	36
Machine diameter	d_m	149.9 mm
Axial length	l_m	70 mm
Rated speed	n_r	$20\,000\text{ min}^{-1}$
Rated torque	M_r	4.8 Nm
Stall torque	M_0	21.2 Nm
Stall current	I_0	70 A
Inverter switching frequency	f_{pulse}	64 kHz

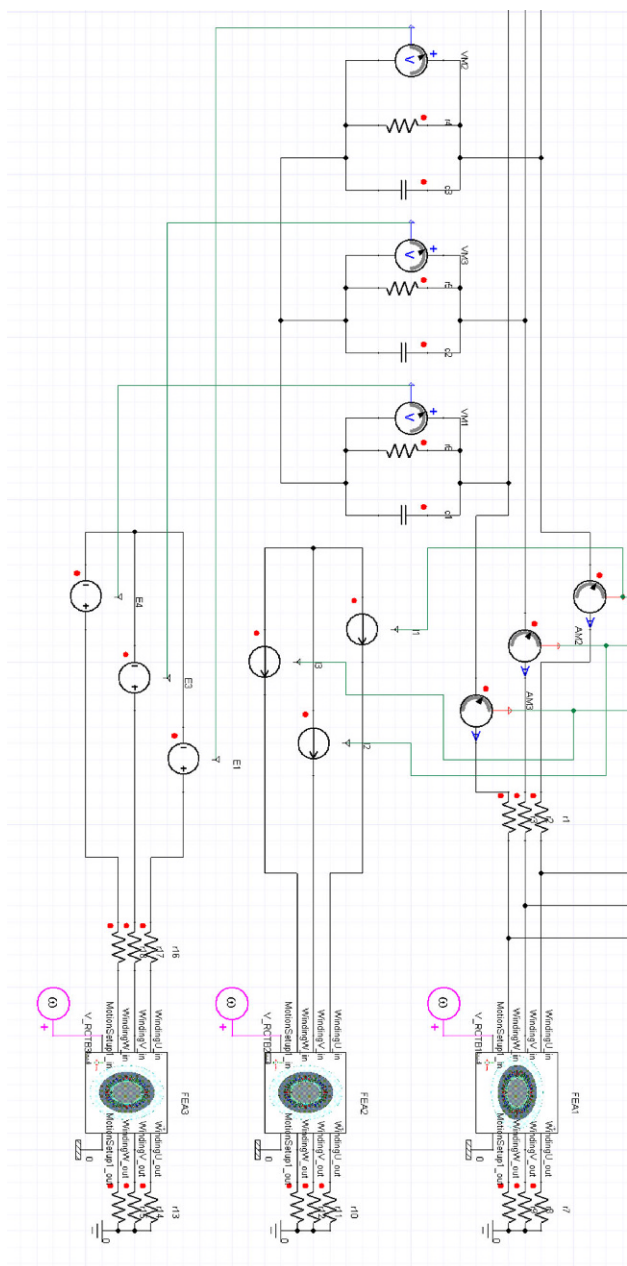


Fig. 4 Cosimulation with three geometrically identical motors and different simulation setups

and its control algorithm are directly coupled to a reference machine without any eddy effects. The controller uses space vector modulation to impress a q-current into the reference machine. The current is then fed into another machine where eddy effects in the permanent magnets are enabled. This is similar to the analytical approaches based on the flux density distribution where a reaction flux is superimposed. The third machine is subjected to the voltage signal of the inverter output. This is closest to the real behavior of the physical machine. An overview of the simulation setup is given in Fig. 4.

The definition of excitation is essential when simulating the effectiveness of a PM segmentation. If the

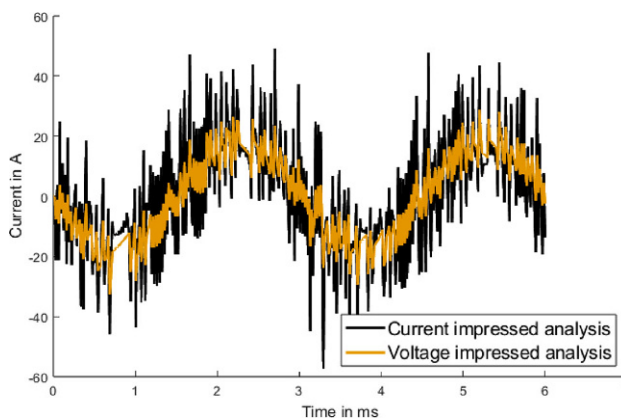


Fig. 5 Simulated currents for current impressed versus voltage impressed analysis

baseline current is used as excitation source, the current linkage remains constant. However, if a voltage signal is fed into the machine, the total flux derivation remains constant. The effect can be observed in the currents, as the eddy current reaction flux dampens the flux in the stator winding. A feedback loop is created when the current increases due to the reduced flux derivation in the winding. Fig. 5 shows the effect of eddy current reaction flux on the current ripple of an inverter-fed SPM with solid permanent magnets.

4.2 Surface permanent magnet machine

Fig. 6 shows the geometry of the analyzed SPM with its parameters given in Table 2. Fig. 7 presents the associated eddy current losses for different numbers of PM segments. The largest deviation between the voltage-impressed simulation and the current-impressed simulation occurs in the region of high eddy current reaction flux, where the number of segments is low and the resistivity of the permanent magnet is also low compared to its reactance. In voltage impressed

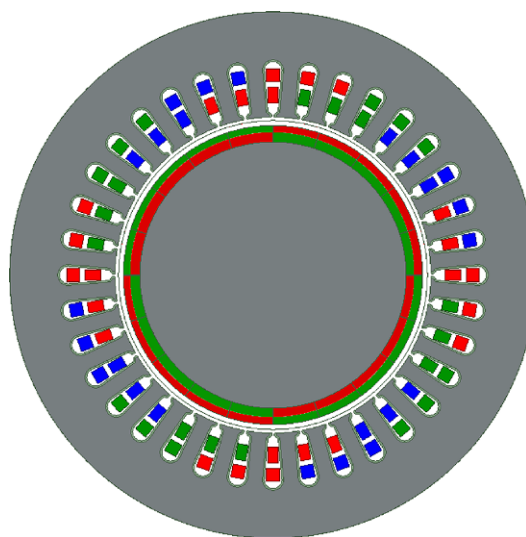


Fig. 6 Cross-section of the simulative analyzed SPM

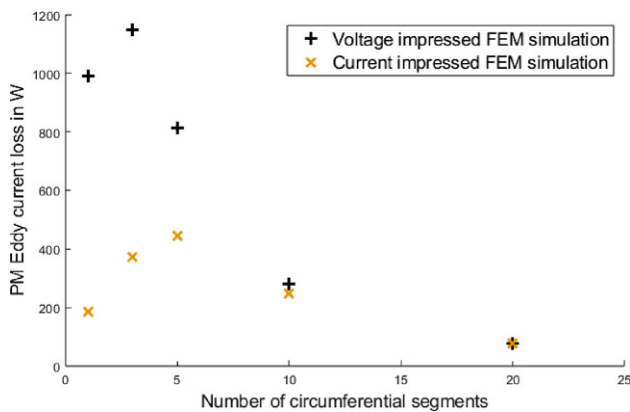


Fig. 7 Eddy current losses in the PM of the SPM for various numbers of segments (current impressed versus voltage impressed simulation)

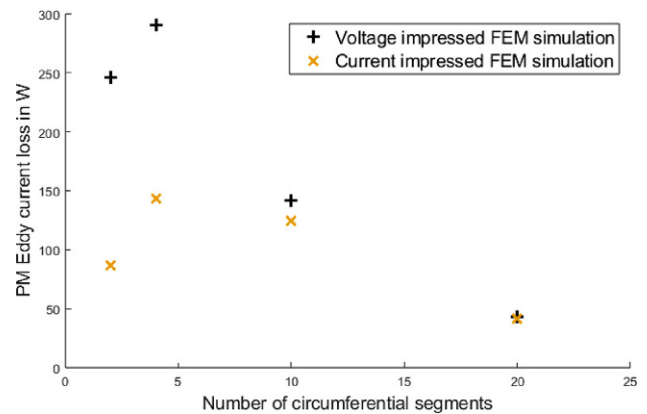


Fig. 9 Eddy current losses in the PM of the IPM for various numbers of segments (current impressed versus voltage impressed simulation)

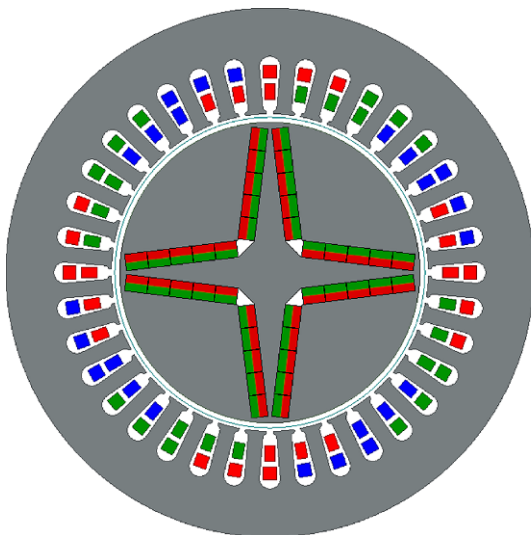


Fig. 8 Cross-section of the simulative analyzed IPM

analysis, the worst-case segmentation with the highest losses is reached at a smaller number of segments than in current impressed analysis. For a large number of segments, eddy currents become resistance limited, reducing the impact of eddy current reaction flux. Both curves eventually converge.

4.3 Interior permanent magnet machine

The geometry of the analyzed IPM is shown in Fig. 8, with its parameters given in Table 2. The design was based solely on the total flux linkage of the fundamental wave. For simulative reasons, the voltage constant of the IPM was identical to the SPM shown in Subsect. 4.2. The design is therefore not intended to be constructed. Overall, the eddy current losses in the PM are lower in the IPM compared to the SPM. This is due to the change in Q-inductance. Similar to the behavior of segmentation in the SPM, the curves deviate for low numbers of segments. However, as shown

in [6], high leakage inductance brings both curves closer together.

5 Conclusion

Eddy current reaction flux behaves differently depending on the excitation source model. In physical rotating electrical machines, there are sources of rotor eddy current losses that must be modeled by a current, namely losses due to slot and winding harmonics, and losses that must be modeled by a voltage, namely inverter-related losses. For losses modeled by a current, the current coupling remains constant. Due to the reaction flux, the total flux decreases. For losses modeled by voltage, the deviation of the total flux linkage must remain constant. The reaction flux displaces the eddy currents but does not reduce the total flux deviation in the winding. Therefore, the current in the winding must increase. State-of-the-art analytical models for eddy current losses in PMSMs are inadequate for modeling all types of eddy current losses in PMs. While they are suitable for slot harmonics and winding harmonics, they cannot accurately model inverter-related losses because they are based on the superposition of the reaction flux, which reduces the total flux linkage deviation. For a large number of segments, the eddy currents are limited by resistance. In this case, the analytical models work well even for inverter-related losses. New models are needed that can facilitate inverter-related losses. The model given in [6] can predict inverter-related eddy current losses in PM, but is not suitable for calculating slot and winding harmonics.

Funding Open Access funding enabled and organized by Projekt DEAL.

Open Access This article is licensed under a Creative Commons Attribution 4.0 International License, which permits use, sharing, adaptation, distribution and reproduction in any medium or format, as long as you give appropriate credit to the original author(s) and the source, provide a link to

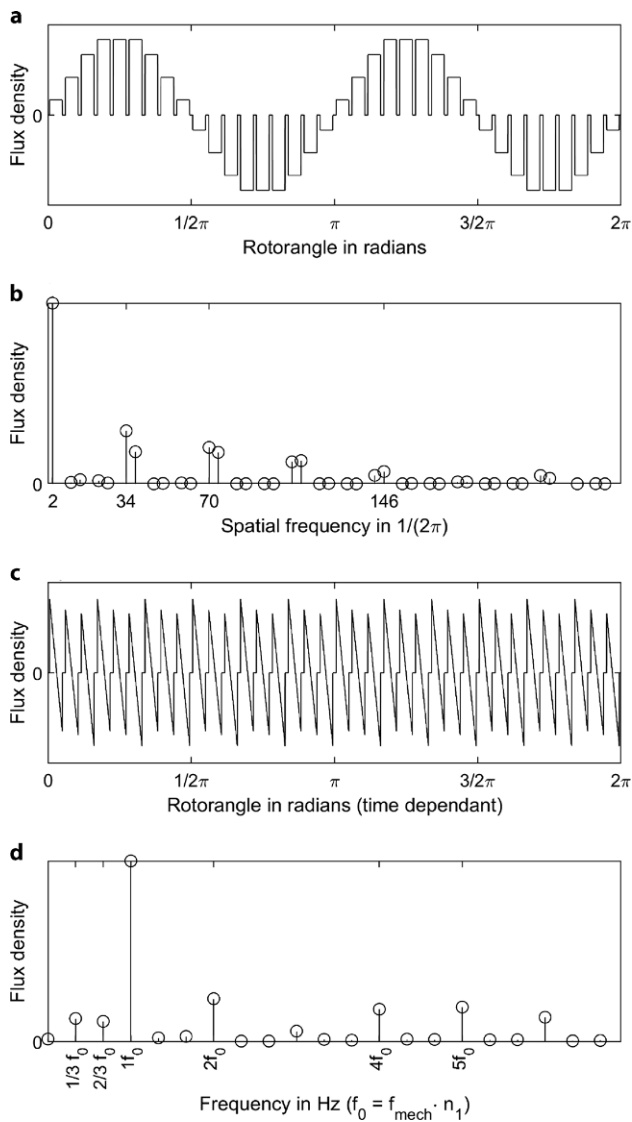


Fig. 10 Synchronous machine with distributed winding (identical to Fig. 6, $p = 2, N_1 = 36$) **a** Stator flux distribution **b** Spatial spectrum of stator flux distribution **c** time dependant rotor flux at reference point **d** time spectrum of rotor flux at reference point

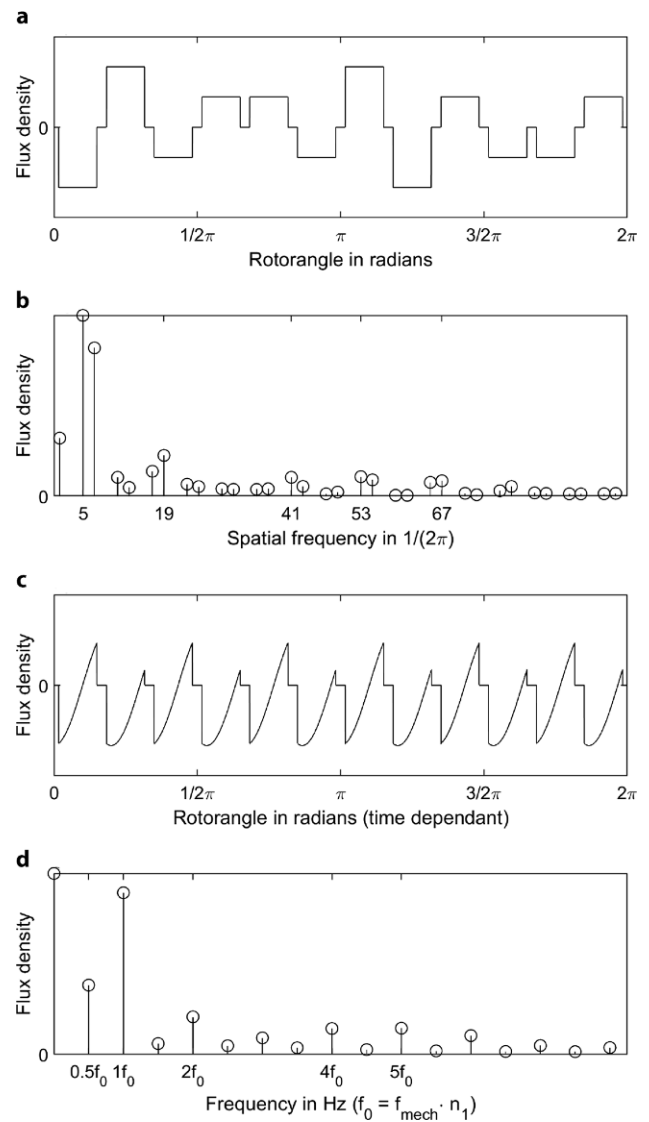


Fig. 11 Synchronous machine with concentrated winding, $p = 5, N_1 = 12$, **a** Stator flux distribution **b** Spatial spectrum of stator flux distribution **c** time dependant rotor flux at reference point **d** time spectrum of rotor flux at reference point

the Creative Commons licence, and indicate if changes were made. The images or other third party material in this article are included in the article's Creative Commons licence, unless indicated otherwise in a credit line to the material. If material is not included in the article's Creative Commons licence and your intended use is not permitted by statutory regulation or exceeds the permitted use, you will need to obtain permission directly from the copyright holder. To view a copy of this licence, visit <http://creativecommons.org/licenses/by/4.0/>.

6 Appendix

6.1 Derivation of rotor reference frame winding harmonics

Let the current in m_1 strands be an ideal sine wave

$$i(t, m) = \hat{I}_q \cdot \cos\left(\omega t + 2\pi \cdot \frac{m-1}{m_1}\right) - \hat{I}_d \cdot \sin\left(\omega t + 2\pi \cdot \frac{m-1}{m_1}\right) = \hat{I}_m \quad (5)$$

with

$$m \in \{1, 2, \dots, m_1\} \quad (6)$$

In each slot N_c corresponding with a tooth N_c there can be N conductors of each of the m_1 stator strands. The calculation of magnetic potentials usually requires some thought about the winding end connections. Usually the engineer takes a look at the winding and adds up all coils enclosing the tooth of interest. However the end connections are not relevant for the magnetic potential. An algorithm can be derived that can calculate the correct magnetic potentials solely based on the current distributions. Starting at any slot we can give the tooth before the slot the magnetic scalar potential $\Psi'_1 = 0A$. The potential of the next slot can then be calculated by adding a virtual mirror current with the value of the sums of the currents of the slot which is located outside of the motor. For a radial flux machine this would represent a toroidally wound machine.

$$\Psi'_{c+1} = \Psi'_c + \sum_1^{m_1} N(m, c) \cdot \underline{i}_m \quad (7)$$

As there is no bias in the currents the sum of the currents is zero, therefore the potential is again zero after a full circle. The magnetic potential differences into the rotor should be symmetrical, therefore the magnetic potential at the rotor should be zero. At the moment the magnetic potential at slot 1 is zero creating a potential gradient throughout the machine. This can be fixed by shifting every potential by an offset.

$$\underline{\Psi}_c = \underline{\Psi}'_c - \frac{\sum_1^{N_1} \underline{\Psi}'_c}{N_1} \quad (8)$$

For simplification the flux distribution under the teeth is assumed to be perfectly rectangular, the flux density under the slot is 0 T and there is a hard cutoff at the edge of the teeth. In reality there are circumferential flux components and there can be a peak in the flux density close to the edges. The magnetic flux distribution due to the winding under one tooth is assumed to be homogeneous and can be calculated based on the magnetic scalar potential difference with the magnetic potential of the rotor being set to zero by the gauging process of Eq. (8).

$$B_n = \mu_0 \frac{Re(\underline{\Psi}_c)}{l_\delta} \quad (9)$$

As the rotor rotates the point of reference moves from one tooth to another. Due to the time dependence of the winding current the magnetic flux under the tooth changes in the time under the tooth as well. The flux density at one point of reference can then be transformed from the time domain to the frequency domain by using the fourier transformation. Examples for the spatial stator flux spectrum and the time dependant rotor flux spectrum at a point of reference are given in Fig. 10 for a distributed winding and in Fig. 11 for a concentrated winding. The ref-

erence point is where the magnetic flux generated by the stator is at the minimum at the point of time and therefore close to the d-axis of the machine. The first graphic a is the airgap flux density in dependance on position at a point in time t . The graphic b is the spatial fourier transform of the airgap flux. Graphic c shows the magnetic flux density at one rotor reference point of the airgap in dependance on the time. As the rotor rotates the currents in the stator windings change aswell. Lastly graphic d shows the time fourier transform of the magnetic flux in the rotor coordinate system at the reference point.

6.2 Nomenclature

p	Number of polepairs
f	Frequency
f_{slot}	Frequency harmonics due to slotting
$f_{winding}$	Frequency harmonics due to winding distribution
f_{inv}	Frequency harmonics due to inverter switching
f_{pulse}	Inverter switching frequency
k	Integer factor for higher order harmonics
M	Torque
n	Rotational speed
N_1	Number of stator slots
m_1	Number of strands
U	Voltage
IPM	Interior permanent magnet machine
PM	Permanent magnet
PMSM	Permanent magnet synchronous machine
SPM	Surface permanent magnet machine

References

1. Yamazaki K, Shina M, Kanou Y, Miwa M, Hagiwara J (2009) Effect of Eddy current loss reduction by segmentation of magnets in synchronous motors: difference between interior and surface types. *IEEE Trans Magn* 45(10):4756–4759. <https://doi.org/10.1109/TMAG.2009.2024159>
2. Yamazaki K, Abe A (2009) Loss investigation of interior permanent-magnet motors considering carrier harmonics and magnet Eddy currents. *IEEE Trans on Ind Applicat* 45(2):659–665. <https://doi.org/10.1109/TIA.2009.2013550>
3. Wakao S, Fujiwara K, Tokumasu T, Kameari A (2005) Useful formulas of analytical investigation in electromagnetic field computation (part 6). In: *Papers Joint Tech. Meeting Static App. Rotating Mach. SA-05-15, RM-05-15. IEE*, pp 83–89 (in Japanese)
4. Sahu R, Pellerey B, Laskaris K (2020) Eddy current loss model unifying the effects of reaction field and non-homogeneous 3-D magnetic field. *IEEE Trans Magn* 56(2):1–4. <https://doi.org/10.1109/TMAG.2019.2953110> (Artno. 7508404)
5. Königs M, Löhlein B (2023) Lumped model for the calculation of harmonic eddy current losses in permanent magnets for homogeneous flux distributions considering eddy current reaction flux. *Elektrotech Inftech*. <https://doi.org/10.1007/s00502-023-01147-z>
6. Königs M, Löhlein B (2023) Lumped model eddy current analysis of influence factors on PM segmentation effective-

- ness. *Elektrotech Inftech*. <https://doi.org/10.1007/s00502-023-01148-y>
7. Huang W-Y, Bettayeb A, Kaczmarek R, Vannier J-C (2010) Optimization of magnet segmentation for reduction of Eddy-current losses in permanent magnet synchronous machine. *IEEE Trans Energy Convers* 25(2):381–387. <https://doi.org/10.1109/TEC.2009.2036250>
 8. Bettayeb A, Jannot X, Vannier J-C (2010) Analytical calculation of rotor magnet eddy-current losses for high speed IPMSM. The XIX International Conference on Electrical Machines – ICEM 2010, Rome, pp 1–6 <https://doi.org/10.1109/ICELMACH.2010.5608257>
 9. Ede JD, Atallah K, Jewell GW, Wang JB, Howe D (2007) Effect of axial segmentation of permanent magnets on rotor loss in modular permanent-magnet Brushless machines. *IEEE Trans on Ind Applicat* 43(5):1207–1213. <https://doi.org/10.1109/TIA.2007.904397>
 10. Mirzaei M, Binder A, Funieru B, Susic M (2012) Analytical calculations of induced Eddy currents losses in the magnets of surface mounted PM machines with consideration of circumferential and axial segmentation effects. *IEEE Trans Magn* 48(12):4831–4841. <https://doi.org/10.1109/TMAG.2012.2203607>
 11. Canders W-R, Bode C, May H (2011) Optimized reduction of parasitic eddy current losses in high speed permanent magnet motors based 2D and 3D field calculations. In: ISEF 2011 – XV Int. Symposium on Electromagnetic Fields in Mechatronics, Electrical and Electronic Engineering Funchal
 12. Thakur S, Odavic M, Allu A et al (2020) Theoretical harmonic spectra of PWM waveforms including dc bus voltage ripple — Application to low-capacitance modular multilevel converter. *IEEE Trans Power Electron* 35(9):9291–9305. <https://doi.org/10.1109/TPEL.2020.2974156>
 13. Jenni F, Wüest D (1995) *Steuerverfahren für selbstgeführte Stromrichter*. vdf Hochschulverlag ETH, Zürich <https://doi.org/10.3929/ethz-a-001427314>

Publisher's Note Springer Nature remains neutral with regard to jurisdictional claims in published maps and institutional affiliations.



Sciences where he is pursuing his Ph.D.

Mike Königs, received his B.Eng. in electrical engineering from the Frankfurt University of Applied Sciences, Germany in 2017 where he enrolled in a dual course of study with the Siemens AG. In 2019 he received his M.Sc. in electrical engineering from the Technical University Kaiserslautern, Germany. After one year in the Test Center Drives with SEW Eurodrive in Bruchsal, Germany he started to work as scientific staff member at the Flensburg University of Applied



Sciences where he is pursuing his Ph.D.

Bernd Löhlein, received his diploma in electrical engineering and information technology from the Technical University Kaiserslautern, Germany in 2007. He completed his doctorate in 2012 and after another six years his habilitation on materials in electrical engineering and mechatronic systems with permanent magnet excited synchronous machines. In 2018 he headed the Chair of Mechatronics and Electrical Drive Systems for one year as a deputy professor. In 2019, Bernd Löhlein became full professor for electrical drive technology at University of Applied Sciences, Flensburg. In 2020 he founded the research group for Innovative Drive Technology in Flensburg. Since 2020, Bernd Löhlein is also external lecturer at Kiel University for electric drives.